Eur. Phys. J. Appl. Phys. (2015) 70: 10901
DOI: 10.1051/epjap/2015150021

THE EUROPEAN PHYSICAL JOURNAL
APPLIED PHYSICS

Regular Article

Statistics of a noise-driven elastic inverted pendulum

Einar Halvorsen[1,a] and Grzegorz Litak[2]

[1] Department of Micro- and Nanosystem Technology, Buskerud and Vestfold University College, Raveien 205, 3184 Borre, Norway
[2] Faculty of Mechanical Engineering, Lublin University of Technology, 20-618 Lublin, Poland

Received: 15 January 2015 / Received in final form: 23 March 2015 / Accepted: 31 March 2015
Published online: 22 April 2015 –

Abstract. Recently an elastic inverted pendulum structure was proposed as a means to make nonlinear energy harvesters. An effective dynamical model of this bi-stable system has an effective lumped mass that is dependent on the displacement, hence preventing direct application of previous analyses for nonlinear harvesters driven by random vibrations. We have set up a stationary Fokker-Planck equation for the inverted pendulum and solved it to obtain explicit expressions for the stationary probability densities of the system. We found that the marginal distribution of velocity is non-Gaussian, but numerically it differs little from a Gaussian when parameters for a recently published device are used. The conditional probability of position given velocity, has two peaks for low velocities. These merge into one upon increase of velocity.

1 Introduction

Vibration energy harvesting is one among several means to provide power to sensor nodes in a way that make them autonomous and thereby allows maintenance free operation [1]. A great number of recent vibration energy harvesters are nonlinear. This is so either because design constraints make linear response unattainable, or because nonlinearities are believed useful in tailoring the device behaviour to the vibration of the environment. Examples of strongly nonlinear devices are found among harvesters of all the three main transducer types, i.e., electromagnetic [2–4], piezoelectric [5–9] and electrostatic [10–14] generators.

In analyzing or testing these devices, a number of different vibration waveforms are used, either measured waveforms or artificial ones. In numerical computations and in experiments, there is a great flexibility in treating different waveforms. For theoretical analyses, simple artificial waveforms such as a pure harmonic vibration or white noise are commonly used because they capture some significant aspects of vibrations and because of the technical difficulties in dealing analytically with the alternatives. With a white-noise excitation that is additive, the probability density of the state variables is given by a Fokker-Planck equation [15] which can be written down rather generally for a harvester with one mechanical degree of freedom and one electrical port [16]. Alternatively one can work directly with the equations of motions for correlation functions. These equations can be solved by several means such as cumulant closure [17], orthogonal function expansions [18,19], equivalent stochastic linearization [20] or finite element methods [21]. Explicit analytical solution for mechanically nonlinear devices [16,22] are achievable in limiting cases of electrical loading when the stationary probability density of velocity and displacement simplifies to the one for a Brownian particle in a potential.

Recently an energy harvester utilizing an elastic inverted pendulum was proposed [23]. The elastic inverted pendulum consists of a thin, vertically oriented beam which can buckle under the gravitational load of a proof mass attached to its end, thereby creating a bistable configuration which can be excited by e.g., horizontal motion of the base. The equations of motion for this system can be reduced to a low-order model with one mechanical degree of freedom. This model has been investigated numerically with harmonic [23–25] and random [26] excitation. The model has the additional complication compared with previous harvester models that the effective lumped mass is dependent on the lateral displacement. This displacement-dependent lumped mass prevents direct application of previous formulations of the Fokker-Planck for energy harvesters with nonlinear stiffness. Since the displacement-dependent lumped mass is a feature of the pendulum structure itself, it is reasonable first to disregard effects of a transducer and focus on the mechanical part of this system in order to gain better understanding of it. In this paper we derive the stationary probability distributions for the effective model of the inverted pendulum.

[a] e-mail: Einar.Halvorsen@hbv.no

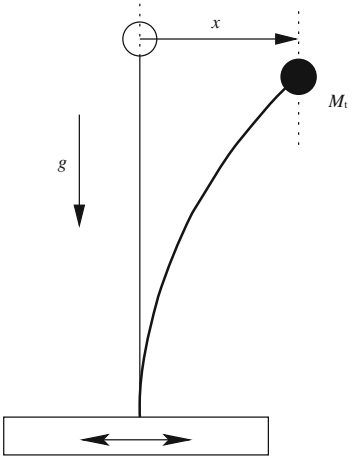

Fig. 1. Main features of the inverted pendulum.

2 The model

The elastic inverted-pendulum configuration is shown in Figure 1 depicting both the reference geometry and an arbitrary state of displacement. The dynamics of the harmonically excited inverted pendulum were studied in previous papers [23,24] where a simplified equation of motion in terms of the tip horizontal displacement was given. The details of the derivation were presented in the reference [23]. It was based on Hamilton's principle using a Lagrangian $T - V$ where the kinetic energy T includes translational kinetic energy of both the beam and tip-mass M_t, as well as the rotational kinetic energy of the tip mass. For the potential energy, the strain energy due to bending and the work done by the gravitational field on the beam and tip-mass were taken into account. The Lagrangian is written in terms of longitudinal and transversal beam displacements $u_p = u_p(s)$ and $v_p = v_p(s)$ respectively as functions of distance s along the beam. Assuming small strains, but not necessarily small displacement, both u_p and the beam curvature can be perturbatively given in terms of v_p so that the Lagrangian is written as a functional of v_p only. The final approximation is to choose an admissible trial function for v_p with the tip-displacement $x = v_p(L)$ as the only free parameter. After expanding the Lagrangian to fourth order in x and $\dot{x}$, the corresponding Euler-Lagrange equation of motion reduces to:

$$(\alpha_1 + \alpha_2 x^2)\ddot{x} + \alpha_2 x\dot{x}^2 + (\gamma_1 + \gamma_2 x^2)x + \beta\dot{x} = F, \quad (1)$$

where F is the fictitious inertial force due to base motion. The parameters α_1 and α_2 parameterize the inertial term which corresponds to a particle with a lumped mass:

$$m(x) = \alpha_1 + \alpha_2 x^2, \quad (2)$$

which is position dependent for nonzero α_2. The effective elastic force corresponds to a potential:

$$U(x) = \gamma_1 x^2/2 + \gamma_2 x^4/4, \quad (3)$$

which has $\gamma_2 > 0$. The configurations of most interest have $\gamma_1 < 0$, and hence (3) is a bistable potential. The damping is treated as a linear damper characterized by a constant β. The parameter values used for numerical examples here are taken from [24] and are listed in Table 1. The potential and lumped mass for these parameters are depicted in Figure 2.

Table 1. Model parameters. Taken from [24].

Parameter	Value	Unit
α_1	0.0294	kg
α_2	1.1094	kg/m^2
γ_1	–0.0633	N/m
γ_2	53.8479	N/m^3
β	0.01	kg/s

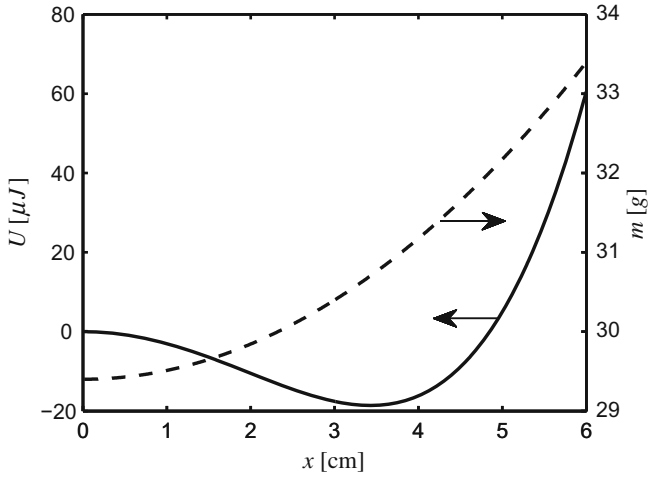

Fig. 2. Potential (full line) and lumped mass (dashed line) vs. displacement. Note that the system has a mirror symmetry. The minimum of the potential is fixed at $x = \pm\sqrt{-\gamma_1/\gamma_2} \approx \pm 3.43$ cm.

We consider a wideband base-excitation which is modeled as a Gaussian-white-noise fictitious force F with autocorrelation function:

$$\langle F(t)F(t')\rangle = S_{FF}\delta(t - t'), \quad (4)$$

where $\langle\cdots\rangle$ denotes the expectation value and δ is the Dirac delta-function. The constant S_{FF} is the (two-sided) spectral density of the force. Note that there are several normalization conventions for the spectral density in the literature, some differing from this one by a factor 2 and/or a factor $1/2\pi$.

3 Probability distributions

In this section we derive the stationary probability density functions for the system and investigate a selection of numerical examples.

3.1 Analytical solutions

We derive the probability densities by setting up and solving a Fokker-Planck equation corresponding to (1).

There are several ways to do this depending on how we choose dynamical variables. We found it most convenient to use the lateral displacement x and its momentum:

$$p = m(x)\dot{x}. \tag{5}$$

For the lossless case ($\beta = 0$) and without base excitation ($F = 0$), the dynamics are then governed by Hamilton's equations $\dot{x} = \partial H/\partial p$ and $\dot{p} = -\partial H/\partial x$ with the Hamiltonian:

$$H(x,p) = \frac{1}{2m(x)}p^2 + U(x). \tag{6}$$

With loss and base-excitation, the equation of motion (1) applies and can be recast as:

$$\dot{x} = \frac{\partial H}{\partial p}, \tag{7}$$

$$\dot{p} = -\frac{\partial H}{\partial x} - \beta\frac{\partial H}{\partial p} + F. \tag{8}$$

We now seek the stationary joint probability density $W_{\rm st} = W_{\rm st}(x,p)$ of displacement and momentum.[1] For the stationary case, the Fokker-Planck equation corresponding to (7), (8) reduces to (see [27], Sect. 4.3):

$$-\frac{\partial}{\partial x}\left(\frac{\partial H}{\partial p}W_{\rm st}\right) + \frac{\partial}{\partial p}\left[\left(\frac{\partial H}{\partial x} + \beta\frac{\partial H}{\partial p}\right)W_{\rm st}\right] + \frac{S_{FF}}{2}\frac{\partial^2 W_{\rm st}}{\partial p^2} = 0. \tag{9}$$

We make the ansatz that the stationary probability distribution only depends on x and p through the Hamiltonian, i.e., $W_{\rm st}(x,p) = f(H(x,p)) = f(H)$ for some function f. This form is motivated by the exact form for an ordinary constant-mass Brownian particle in a potential. In our case this ansatz turns out to work for the joint probability density of x and p, but in contrast to the constant-mass case [28], it can then not work for the probability density of x and $\dot{x}$.

Inserting the ansatz into (9), we obtain:

$$\frac{\partial^2 H}{\partial p^2}\left[f' + \frac{2\beta}{S_{FF}}f\right] + \left(\frac{\partial H}{\partial p}\right)^2\left[f'' + \frac{2\beta}{S_{FF}}f'\right] = 0. \tag{10}$$

As both terms in brackets must vanish, the solution to this equation indeed must be on the form $f \propto \exp(-2\beta H/S_{FF})$, i.e., a Boltzmann factor with $2\beta/S_{FF}$ analogous to the reciprocal of temperature. We therefore have:

$$W_{\rm st} = Z^{-1}\exp\left(-\frac{\beta}{S_{FF}}\frac{p^2}{m(x)} - \frac{2\beta}{S_{FF}}U(x)\right), \tag{11}$$

where

$$Z = \int_{-\infty}^{\infty}{\rm d}x\int_{-\infty}^{\infty}{\rm d}p\ \exp\left(-\frac{\beta}{S_{FF}}\frac{p^2}{m(x)} - \frac{2\beta}{S_{FF}}U(x)\right), \tag{12}$$

ensures correct normalization of the probability density. The x-dependence in (11) is the same as would have been obtained by simply replacing the mass by a spatially varying one in the expression for the probability density for an ordinary constant-mass Brownian particle. However, the normalization factor is different for that case.

If we instead seek the joint probability density $\tilde{W}_{\rm st} = \tilde{W}_{\rm st}(x,\dot{x})$ of displacement and velocity, we can make a change of variables to find $\tilde{W}_{\rm st}(x,\dot{x}) = m(x)W_{\rm st}(x,m(x)\dot{x})$, i.e.,

$$\tilde{W}_{\rm st} = Z^{-1}m(x)\exp\left(-\frac{\beta}{S_{FF}}m(x)\dot{x}^2 - \frac{2\beta}{S_{FF}}U(x)\right). \tag{13}$$

In contrast to the constant-mass case, velocity and position are no longer independent stochastic variables, but their equal-time covariance is $\langle x\dot{x}\rangle = 0$ as it should.

The marginal probability density $W_{x,\rm st}$ for position can be found by integrating out either momentum in (11) or velocity in (13). The result is:

$$W_{x,\rm st}(x) = Z^{-1}\sqrt{\frac{\pi S_{FF}m(x)}{\beta}}\exp\left(-\frac{2\beta}{S_{FF}}U(x)\right). \tag{14}$$

The marginal probability density $W_{\dot{x},\rm st}$ for velocity is similarly obtained by integrating out the displacement in (13). For the form of $m(x)$ and $U(x)$ in (2) and (3), we obtain the explicit result:

$$\begin{aligned} W_{\dot{x},\rm st}(\dot{x}) = {} & Z^{-1}\sqrt{\pi}\left(\frac{S_{FF}}{\beta\gamma_2}\right)^{\frac{1}{4}}\exp\left(-\frac{\beta\alpha_1}{S_{FF}}\dot{x}^2\right) \\ & \times\exp\left(\frac{\beta}{4S_{FF}\gamma_2}(\gamma_1+\alpha_2\dot{x}^2)^2\right) \\ & \times\left[\alpha_1 D_{-\frac{1}{2}}\left(\sqrt{\frac{\beta}{S_{FF}\gamma_2}}(\gamma_1+\alpha_2\dot{x}^2)\right)\right. \\ & \left.+\frac{\alpha_2}{2}\sqrt{\frac{S_{FF}}{\beta\gamma_2}}D_{-\frac{3}{2}}\left(\sqrt{\frac{\beta}{S_{FF}\gamma_2}}(\gamma_1+\alpha_2\dot{x}^2)\right)\right], \end{aligned} \tag{15}$$

where $D_{-\frac{1}{2}}$ and $D_{-\frac{3}{2}}$ are parabolic cylinder functions [29].

3.2 Examples

The expression for the marginal probability density of velocity (15) appears quite different from the Gaussian distribution one would have if the lumped mass did not depend on displacement. We plotted it for $S_{FF} = 1.0\times 10^{-6}$ N^2/Hz in Figure 3 compared to the Gaussian distribution resulting from setting $\alpha_2 = 0$. The effect of the displacement-dependent lumped mass is in this case a heightening and narrowing of the distribution. That this effect is rather small, is understandable in this case because the lumped mass changes only with a few percent within the double well as seen from Figure 2. We would need a mass-variation with displacement that is significant within the probable displacement-range in order to

[1] As is common in physics and engineering, we use the same notation for the dummy variables in the probability distributions as for the corresponding stochastic variables, i.e., x and $\dot{x}$.

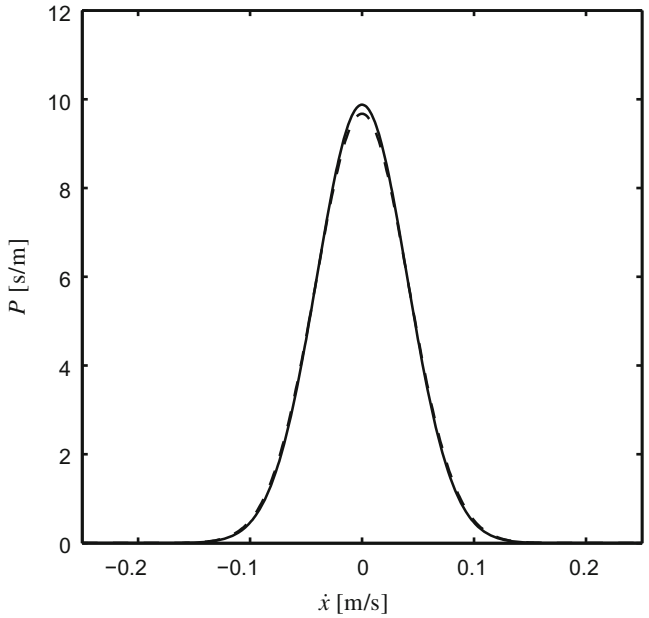

Fig. 3. Marginal probability distribution of velocity: $\alpha_2 = 1.1094$ kg/m^2 (full line) and $\alpha_2 = 0$ (dashed line).

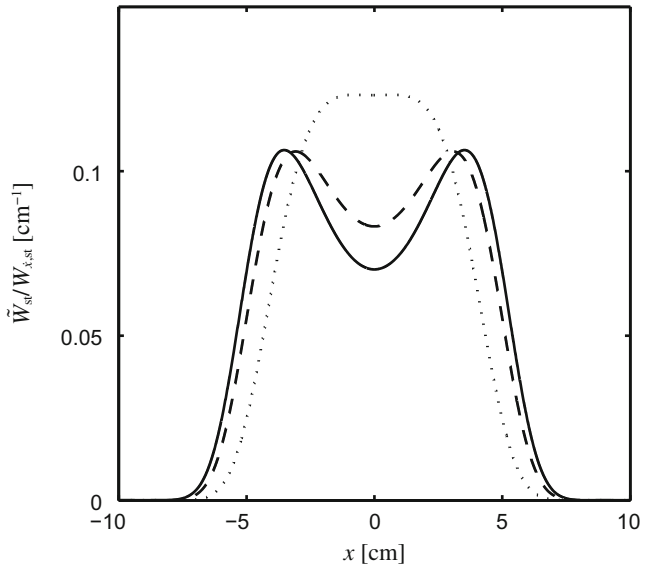

Fig. 4. Conditional probability distribution of displacement $\tilde{W}_{\rm st}(x,\dot{x})/W_{\dot{x},\rm st}(\dot{x})$ for velocities $\dot{x} = 0$ m/s (solid line), 0.12 m/s (dashed line) and 0.24 m/s (dotted line).

have a large effect. This is not the case for this particular device. From the expression (14), we see that also the marginal distribution for the displacement will have this feature.

Since the velocity and displacement are not statistically independent when the lumped mass is displacement-dependent, we might expect a stronger effect in the joint probability distribution for x and $\dot{x}$ than for the marginal distributions of either quantity, or alternatively in the conditional probabilities. The exponent in (13) is proportional to the energy which can be written:

$$E(x,\dot{x}) = H(x, m(x)\dot{x}) = \frac{1}{2}\alpha_1\dot{x}^2 + \frac{1}{2}(\gamma_1 + \alpha_2\dot{x}^2)x^2 + \frac{1}{4}\gamma_2 x^4, \quad (16)$$

for the inverted pendulum. The middle term is zero when $|\dot{x}| = \sqrt{-\gamma_1/\alpha_2} \approx 0.2389$ m/s and we could expect an effective lowering of the barrier on the high-velocity tails of the distribution. This is the case and is illustrated in Figure 4 which shows the conditional probability density of displacement given the velocity, i.e., $\tilde{W}_{\rm st}(x,\dot{x})/W_{\dot{x},\rm st}(\dot{x})$, for $S_{FF} = 1.0 \times 10^{-6}$ N^2/Hz and three velocities. For a position-independent lumped mass all three cases should be equal. Here we see that for $\dot{x} = 0$, we have the double-peak structure that is typical for the bistable potential. With increasing velocity these peaks tend to merge and at $\dot{x} = 0.24$ m/s the double-peak structure almost vanished. The full probability distribution is shown in Figure 5.

For better clarity regarding the system response, we solved (1) numerically. The corresponding Langevin equation as a first-order system of stochastic differential

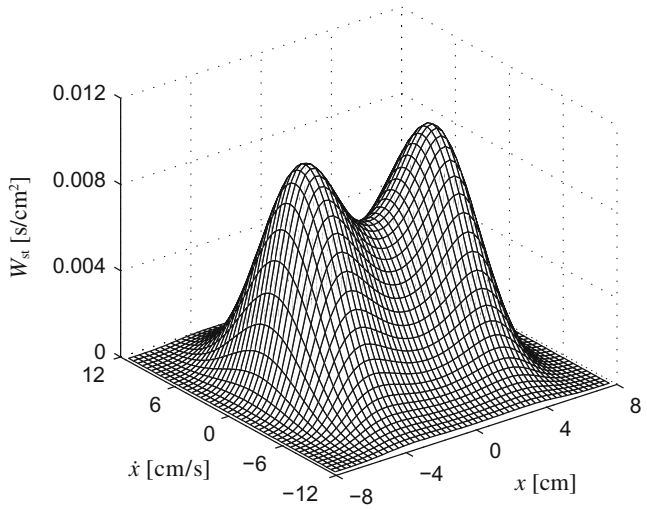

Fig. 5. Stationary probability distribution $\tilde{W}_{\rm st}(x,\dot{x})$.

equations was written:

$$\dot{x} = v, \quad (17)$$

$$\dot{v} = \frac{-\alpha_2 x v^2 - (\gamma_1 + \gamma_2 x^2)x - \beta v + F}{\alpha_1 + \alpha_2 x^2}. \quad (18)$$

After time discretization, we performed the numerical integration via Runge-Kutta-Maruyama algorithm [30,31].

The results of numerical simulations are presented in Figure 6. Both time history (Fig. 6a) and phase portrait (Fig. 6b) show the solution characterized by hopping between the symmetric potential wells.

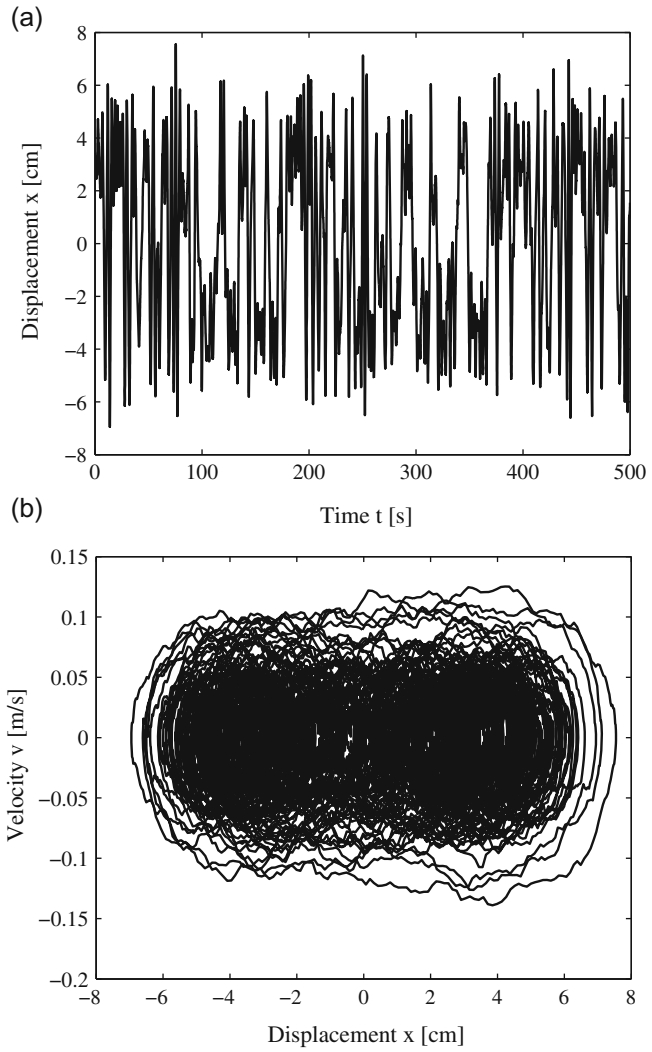

Fig. 6. Time history of displacement (a) and phase portrait (b) of the noise-driven pendulum with $S_{FF} = 1.0 \times 10^{-6}$ N^2/Hz.

4 Conclusion

We formulated and solved a Fokker-Planck equation for an elastic inverted pendulum based on a previously derived equation of motion for the system. The form of the joint probability distributions turns out to be simply the ones of a Brownian particle in potential with its constant mass replaced by the position-dependent one. The marginal distribution of velocity is not Gaussian as in the constant-mass case, but can be expressed in terms of parabolic cylinder functions. The conditional probability density of position for given velocity displays a change from a two-peak distribution characteristic of a bi-stable potential potential to a single-peak function as velocity increases from zero. The analytic expressions for the probability densities obtained here may be useful for further development of an analytic treatment of the noise-driven inverted-pendulum-based energy harvester.

G. Litak gratefully acknowledges the support of the Polish National Science Center under Grant No. 2012/05/B/ST8/00080. E. Halvorsen was supported by the Research Council of Norway under Grant No. 229716/E20.

References

1. P.D. Mitcheson, E.M. Yeatman, G.K. Rao, A.S. Holmes, T.C. Green, Proc. IEEE **96**, 1457 (2008)
2. S. Burrow, L. Clare, A Resonant Generator with Non-Linear Compliance for Energy Harvesting in High Vibrational Environments, in *2007 IEEE International Electric Machines Drives Conference, IEMDC '07*, vol. 1 (Antalya, Turkey, 2007), pp. 715–720
3. M.S.M. Soliman, E.M. Abdel-Rahman, E.F. El-Saadany, R.R. Mansour, J. Micromech. Microeng. **18**, 115021 (2008)
4. B. Mann, N. Sims, J. Sound Vib. **319**, 515 (2009)
5. A. Erturk, J. Hoffmann, D.J. Inman, Appl. Phys. Lett. **94**, 254102 (2009)
6. S.C. Stanton, C.C. McGehee, B.P. Mann, Appl. Phys. Lett. **95**, 174103 (2009)
7. F. Cottone, H. Vocca, L. Gammaitoni, Phys. Rev. Lett. **102**, 080601 (2009)
8. M. Marzencki, M. Defosseux, S. Basrour, J. Microelectromech. Syst. **18**, 1444 (2009)
9. G. Sebald, H. Kuwano, D. Guyomar, B. Ducharne, Smart Mater. Struc. **20**, 075022 (2011)
10. P. Miao, P.D. Mitcheson, A.S. Holmes, E.M. Yeatman, T.C. Green, B.H. Stark, Microsys. Technol. **12**, 1079 (2006)
11. D. Miki, M. Honzumi, Y. Suzuki, N. Kasagi, Large-amplitude MEMS electret generator with nonlinear spring, in *IEEE 23rd International Conference on Micro Electro Mechanical Systems (MEMS 2010), 2010*, pp. 176–179
12. L.G.W. Tvedt, D.S. Nguyen, E. Halvorsen, J. Microelectromech. Syst. **19**, 305 (2010)
13. C.P. Le, E. Halvorsen, O. Søråsen, E.M. Yeatman, J. Intell. Mater. Syst. Struct. **23**, 1409 (2012)
14. S.D. Nguyen, E. Halvorsen, I. Paprotny, Appl. Phys. Lett. **102**, 023904 (2013)
15. H. Risken, *The Fokker–Planck Equation: Methods of Solutions and Applications*, Springer Series in Synergetics, 2nd edn., vol. 18 (Springer-Verlag, New York, 1996)
16. E. Halvorsen, J. Microelectromech. Syst. **17**, 1061 (2008)
17. M.F. Daqaq, Nonlinear Dyn. **69**, 1063 (2012)
18. E. Halvorsen, S.D. Nguyen, in *Advances in Energy Harvesting Methods*, edited by N. Elvin, A. Erturk (Springer, New York, 2013), pp. 63–90
19. W. Martens, U. Wagner, G. Litak, Eur. Phys. J. Special Top. **222**, 1665 (2013)
20. I.L. Cassidy, J.T. Scruggs, Smart Mater. Struc. **21**, 085003 (2012)
21. P. Kumar, S. Narayanan, S. Adhikari, M. Friswell, J. Sound Vib. **333**, 2040 (2014)
22. L. Gammaitoni, I. Neri, H. Vocca, Appl. Phys. Lett. **94**, 164102 (2009)
23. M.I. Friswell, S.F. Ali, O. Bilgen, S. Adhikari, A.W. Lees, G. Litak, J. Intell. Mater. Syst. Struct. **23**, 1505 (2012)

24. G. Litak, M. Coccolo, M.I. Friswell, S.F. Ali, S. Adikari, A.W. Lees, O. Bilgen, Nonlinear Oscillations of an Elastic Inverted Pendulum, in *4th IEEE International Conference on Nonlinear Science and Complexity – NSC 2012* (Budapest, Hungary, 2012), pp. 113–116
25. O. Patil, P. Gandhi, J. Dyn. Syst. Meas. Control **136**, 041017 (2014)
26. M. Borowiec, G. Litak, M.I. Friswell, S.F. Ali, S. Adhikari, A.W. Lees, O. Bilgen, International Journal of Structural Stability and Dynamics **13**, 1340006 (2013)
27. C.W. Gardiner, *Handbook of Stochastic Methods*, Springer series in Synergetics, 3rd edn., vol. 13 (Springer-Verlag, Berlin Heidelberg, 2004)
28. S. Mongkolsakulvong, T.D. Frank, Condensed Matter Physics **13**, 13001 (2010)
29. M. Abramowitz, I.A. Stegun, *Handbook of Mathematical Functions* (Dover, New York, 1970)
30. A. Naess, V. Moe, Prob. Eng. Mech. **15**, 221 (2000)
31. G. Litak, M. Friswell, S. Adhikari, Appl. Phys. Lett. **96**, 214103 (2010)